

DESY 93-035  
 BI-TP 93/09  
 March 1993  
 Phys. Letters B308 (1993) 403  
 revised July 1995

# Off-shell $W$ -pair production in $e^+e^-$ -annihilation

## – *Initial state radiation* –

D. Bardin <sup>1,2</sup>, M. Bilenky <sup>1,2</sup>, A. Olchevski <sup>2a</sup> and T. Riemann <sup>1</sup>

<sup>1</sup> DESY – Institut für Hochenergiephysik  
 Platanenallee 6, D-15738 Zeuthen, Germany

<sup>2</sup> Bogoliubov Laboratory for Theoretical Physics, JINR  
 ul. Joliot-Curie 6, RU-141980 Dubna, Moscow Region, Russia

### ABSTRACT

With a current-splitting technique, we calculate the gauge-invariant initial-state radiation to order  $\mathcal{O}(\alpha)$  with soft-photon exponentiation for on- and off-shell  $W$ -pair production. This result generalizes the convolution formula, which is known from the description of the  $Z$  resonance, to the case of the production of two  $W$ -bosons. After up to eightfold analytical integrations, a sufficiently smooth integral over three invariant masses remains to be treated numerically. Including the Coulomb singularity, the largest corrections are covered. We discuss the corrections in a large energy range up to  $\sqrt{s}=1$  TeV and draw numerical conclusions on their influence on the  $W$ -mass determination at LEP 200.

Table 1 and figure 5 are revised after correcting the analytical formulae for the nonuniversal corrections.

---

<sup>a</sup> Present address: CERN, Geneva, Switzerland

email: BARDINDY@CERNVM.CERN.CH, BILENKYM@VXCERN.CERN.CH,  
 OLSHEVSK@VXCERN.CERN.CH, riemann@ifh.de

# 1 Introduction

The Standard Model of electroweak interactions allows the calculation of the width  $\Gamma_W$  [1] and mass  $M_W$  of the  $W$  boson; the latter may be iterated from  $\Delta r$  [2], the electroweak correction to the muon decay constant. For fixed  $t$ -quark and Higgs masses, the predictions of the Standard Model are much more precise than the available experimental data.

A direct measurement of  $\Gamma_W$  and  $M_W$  will be one of the main tasks of LEP 200 [3, 4]. This will be possible from a study of the reaction

$$e^+e^- \rightarrow (W^+W^-) \rightarrow 4f, \quad (1)$$

which is accompanied by the emission of photons [5] and gluons,

$$e^+e^- \rightarrow 4f + n_1\gamma + n_2g. \quad (2)$$

The photons may be emitted by the initial and intermediate states; and both photons and gluons by final state particles. With a centre-of-mass energy at LEP 200 of  $\sqrt{s} \approx 190$  GeV, the  $W$ -pair production proceeds near the threshold. Thus, the finite width effects in the off-shell production must be taken into account. And last but not least, virtual electroweak corrections have to be inserted properly.

Here, we will concentrate on the treatment of *Initial State Radiation* (ISR) <sup>1</sup>. The aim is to obtain (semi-)analytical expressions for the total cross section at LEP 200, but also at higher energies [7, 8]. In section 2, we introduce the Born cross section and define the notations. In section 3, photonic bremsstrahlung will be faced. Since the  $W$ -boson is electrically charged, we have to derive properly a gauge-invariant definition of ISR. Section 4 contains the cross section formulae with contributions from ISR. For the applications at LEP 200, we discuss in section 5 a possible estimate of the Coulomb singularity. Numerical results and some conclusions both for LEP 200 and for a wide energy range are presented in section 6.

## 2 The Born cross section

The main contributions to reaction (1) are shown in figure 1: two **crayfish** diagrams and one **crab** diagram. We use the unitary gauge; in a non-unitary gauge, one should have to take into account additional diagrams. The cross section is well described by a twofold convolution of a hard-scattering off-shell cross section [9]:

$$\sigma_B^{\text{off}}(s) = \int_0^s ds_1 \rho(s_1) \int_0^{(\sqrt{s}-\sqrt{s_1})^2} ds_2 \rho(s_2) \sigma_0(s; s_1, s_2), \quad (3)$$

$$\rho(s_i) = \frac{1}{\pi} \frac{\sqrt{s_i} \Gamma_W(s_i)}{|s_i - M_W^2 + i\sqrt{s_i} \Gamma_W(s_i)|^2} \times \text{BR}(i), \quad (4)$$

$$\Gamma_W(s_i) = \sum_f \frac{G_\mu M_W^2}{6\pi\sqrt{2}} \sqrt{s_i}. \quad (5)$$

---

<sup>1</sup>In another article [6], we classify and study several background reactions with the same signature as (1), but different intermediate states. They have to be added in order to ensure gauge invariance for the process.

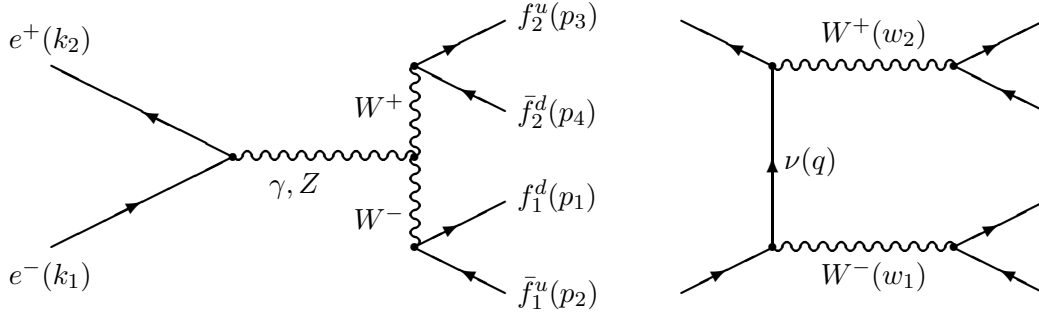


Figure 1: *The Feynman diagrams for off-shell  $W$ -pair production: **crayfish** and **crab**.*

The off-shell width  $\Gamma_W(s_i)$  contains a sum over all open fermion-decay channels  $f$  at energy  $\sqrt{s_i}$ , and  $\text{BR}(i)$  is the corresponding branching fraction. We have rederived the results of [9] and refer for details to that article. For later use, we split the cross section into three pieces:

$$\sigma_0 = \sigma_0^s + \sigma_0^{\text{st}} + \sigma_0^t. \quad (6)$$

### 3 Photonic corrections to $W$ -pair production

In the description of the complicated scattering process (2), it seems to be desirable to find gauge-invariant subsets of Feynman diagrams. Further, one would like to separate in a reasonable way the terms related to bremsstrahlung from the genuine electroweak virtual corrections.

A procedure to disentangle final-state real photon emission from the rest of the process (2) has been proposed in [10]. A corresponding separation of virtual photonic corrections should be performed in parallel. In the presence of  $W$  exchange, these do not form a gauge-invariant subset of diagrams. Being mainly interested in real bremsstrahlung, one could decide to combine it only with the singular parts of the virtual diagrams [11]. The singular parts are then uniquely defined up to an additive constant and will compensate the singularities of the real bremsstrahlung.

These few remarks should indicate that there is much work to be done if one intends to perform a systematic, semi-analytical study of reaction (2). For a Monte-Carlo approach, we refer to [5].

In the following, we will concentrate on ISR. Thus, we avoid to be faced with the full complexity of the problems, and at the same time we will cover the bulk of the numerically important corrections. The initial-state radiation offers no problems in the case of radiation from the **crayfish** diagrams. Here, the initial charges are separated by the exchange of neutral gauge bosons from the rest of the diagrams, and ISR is well-defined.

#### 3.1 The $t$ -channel ISR problem – splitting the neutrino current

The **crab** diagram contains a neutrino exchange in the  $t$  channel. The photonic corrections to the initial state are shown in figure 2.

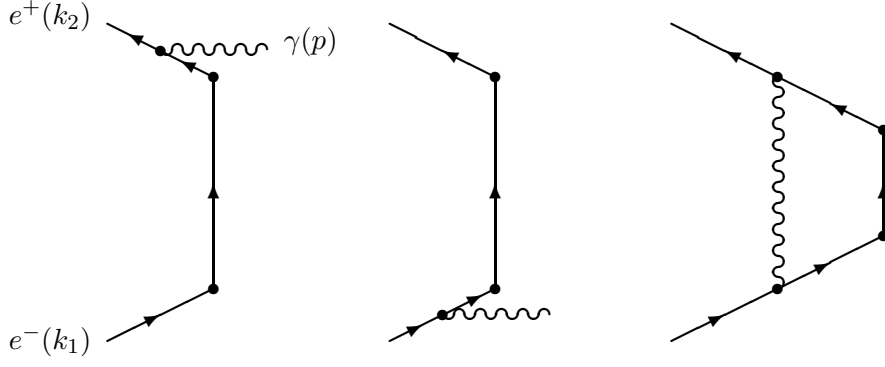


Figure 2: *The usual initial-state photonic corrections to the crab diagram.*

The bremsstrahlung may be described by the following electromagnetic current:

$$\mathcal{J}_{\mu,\alpha\beta}^{\text{br}} = Q_e \bar{u}(k_2) \left[ \gamma_\alpha \frac{\hat{w}_2 - \hat{k}_2}{(w_2 - k_2)^2} \gamma_\beta \frac{2k_1^\mu - \hat{p} \gamma_\mu}{-2k_1 p} - \frac{2k_2^\mu - \gamma_\mu \hat{p}}{-2k_2 p} \gamma_\alpha \frac{-\hat{w}_1 + \hat{k}_1}{(w_1 - k_1)^2} \gamma_\beta \right] (1 + \gamma_5) u(k_1), \quad (7)$$

where the  $\{k_1, k_2, p, w_1, w_2\}$  are the four-momenta of  $\{e^-, e^+, \gamma, W^-, W^+\}$ , respectively. This current is not conserved,  $p^\mu \mathcal{J}_{\mu,\alpha\beta}^{\text{br}} \neq 0$ , and gauge-invariance is violated. Nevertheless, one may construct a conserved current also for the **crab** diagram. Intuitively, it is evident that one has to allow the flow of charge *within* the initial state; a charge  $Q_e$  has to be associated to the neutrino propagator. This, in turn, enables the neutrino to radiate, see figure 3. The resulting auxiliary current,

$$\mathcal{J}_{\mu,\alpha\beta}^{\text{aux}} = Q_e \bar{u}(k_2) \left[ \gamma_\alpha \frac{\hat{w}_2 - \hat{k}_2}{(w_2 - k_2)^2} \gamma_\mu \frac{-\hat{w}_1 + \hat{k}_1}{(w_1 - k_1)^2} \gamma_\beta \right] (1 + \gamma_5) u(k_1), \quad (8)$$

ensures current conservation in the initial state and thus makes the d combined diagrams gauge-invariant. In fact, the net initial-state current,

$$\mathcal{J}_{\mu,\alpha\beta}^{\text{ini}} \equiv \mathcal{J}_{\mu,\alpha\beta}^{\text{br}} + \mathcal{J}_{\mu,\alpha\beta}^{\text{aux}}, \quad (9)$$

fulfills current conservation,

$$p^\mu \mathcal{J}_{\mu,\alpha\beta}^{\text{ini}} = 0. \quad (10)$$

In order to compensate for the extra piece in the matrix element, one has to add also a diagram with flow of charge  $-Q_e$  through the neutrino propagator, which in its turn has to be combined with the charge flow through the  $W$  bosons to build also a continuous electric charge flow – but now as part of the *intermediate state* of the process (or, in case of on-shell  $W$ -pair production, of the final state). In effect, the electrically neutral neutrino has been split into two oppositely flowing, equal charges <sup>2</sup>.

---

<sup>2</sup>For quarks, the auxiliary diagrams from the ‘charged’ neutrino are naturally present, and by no means auxiliary. For an application of the CST in  $ep$  scattering at HERA, see [11].

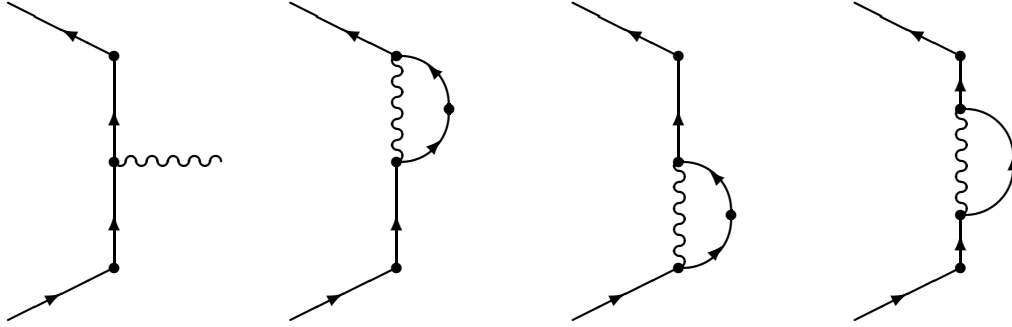


Figure 3: *The auxiliary initial-state photonic corrections to the crab diagram.*

For this reason, we call this method of restoring gauge invariance for ISR the *Current Splitting Technique* (CST).

The introduction of an additional bremsstrahlung diagram to ISR has a further consequence: one must take into account also additional virtual corrections. These are also shown in figure 3. They, together with the corresponding counter terms, will ensure the compensation of the infrared divergencies of the photon radiation from the beam particles. The counter terms also cancel the UV-divergencies of the newly introduced virtual corrections. The additional radiation from the neutrino line is free of any infrared divergency, since the radiating particle is off-shell.

## 4 Initial-state radiation

For the  $s$ -channel **crayfish** diagram we rederived the ISR correction factor, which is well-known from  $Z$ -resonance calculations; see e.g. [12] and references cited therein. The corresponding cross section is described by a threefold convolution:

$$\frac{d^2\sigma_s}{ds_1 ds_2} = \int_{(\sqrt{s_1} + \sqrt{s_2})^2}^s \frac{ds'}{s} \left[ \beta_e v^{\beta_e - 1} (1 + \bar{S}) + \bar{H} \right] \rho(s_1) \rho(s_2) \sigma_0^s(s'; s_1, s_2). \quad (11)$$

Here, it is  $v = 1 - s'/s$  and the soft plus virtual photon part  $\bar{S}(s)$  and hard part  $\bar{H}(s, s')$  are:

$$\bar{S}(s) = \frac{\alpha}{\pi} \left[ \frac{\pi^2}{3} - \frac{1}{2} \right] + \frac{3}{4} \beta_e + \mathcal{O}(\alpha^2), \quad \bar{H}(s, s') = -\frac{1}{2} \left( 1 + \frac{s'}{s} \right) \beta_e + \mathcal{O}(\alpha^2), \quad (12)$$

and  $\beta_e = 2\alpha/\pi [\ln(s/m_e^2) - 1]$ .

### 4.1 The ISR connected with the crab diagram

For a treatment of single-photon bremsstrahlung, one has to integrate a tenfold distribution. The degrees of freedom of the four-fermion final state have been chosen to be two pairs of angles in the rest systems of the two fermion pairs. These integrations are trivially performed with the method of tensor integration (see e.g. [13]). As further integration variables, we took the cosine of the photon angle  $\theta_\gamma$  in the centre-of-mass system and the two angles  $\phi_W, \theta_W$  of

the virtually produced  $W^-$ -boson in the recoil system, i.e. with respect to the photon axis. It is the integration over these three angles which demands some effort, and which leads to the tremendous complications in the case of the **crab** diagram with a neutrino exchange in the  $t$  channel.

Details of the calculation will be published elsewhere. The algebraic manipulations have been performed with the aid of the programs for algebraic manipulations **SCHOONSCHIP** and **FORM** [14]. We finally arrived at the following cross section:

$$\frac{d^2\sigma_a}{ds_1 ds_2} = \int_{(\sqrt{s_1}+\sqrt{s_2})^2}^s \frac{ds'}{s} \rho(s_1) \rho(s_2) \left[ \beta_e v^{\beta_e-1} \mathcal{S}_a + \mathcal{H}_a \right], \quad (13)$$

$$\mathcal{S}_a(s, s'; s_1, s_2) = \left[ 1 + \bar{S}(s) \right] \sigma_0^a(s'; s_1, s_2) + \sigma_{\bar{S}}^a(s'; s_1, s_2), \quad (14)$$

$$\mathcal{H}_a(s, s'; s_1, s_2) = \bar{H}(s, s') \sigma_0^a(s'; s_1, s_2) + \sigma_{\bar{H}}^a(s, s'; s_1, s_2). \quad (15)$$

Here,  $a=st, t$  denote the  $st$ -interference and  $t$ -channel contributions, respectively. The functions  $\mathcal{S}_a(s, s'; s_1, s_2)$  and  $\mathcal{H}_a(s, s'; s_1, s_2)$  contain extra cross-section pieces with deviations from the structure of the  $s$ -channel case. As already mentioned, they are *nonuniversal* in the sense that they differ for  $a=st, t$ . Further, they are *not factorizing*, i.e. they do not contain the off-shell Born cross section as an explicit factor. A third feature of them is a *screening* property: compared to the Born cross section, they have a damping overall factor,

$$\sigma_{\bar{S}, \bar{H}}^{st, t}(s'; s_1, s_2) \sim \frac{s_1 s_2}{s^2}, \quad (16)$$

which suppresses potential mass singularities, which otherwise would be generated by new kinematic logarithms compared to the Born cross section. The non-universality of the additional corrections could, in principle, spoil the *gauge cancellations* [15] between the three diagrams of figure 1. From the analytical structure of the nonuniversal terms, such a cancellation may not be seen; the  $\sigma_{\bar{S}, \bar{H}}^a(s'; s_1, s_2)$  are complicated functions, as one may expect after seven to eight integrations. The property (16) is welcome in this respect, but it could be compensated at least partly by the integrations over invariant masses; numerically, we have observed that the net cross section behaves properly at extremely high energies. A consequence of the auxiliary current is that our formulae for ISR contain some contributions which in other calculations are considered a part of the *intermediate or final-state radiation*.

Besides rational functions and logarithms of  $s, s', s_1, s_2$ , they contain dilogarithms and, in case of the virtual corrections, trilogarithms. We will publish the explicit expressions for the cross section elsewhere. Despite the fact that they are relatively lengthy, we would like to stress that they are much more compact than they would be without the introduction of the auxiliary current (8). It is of importance for a numerical handling that the  $\sigma_{\bar{S}}^a$  and  $\sigma_{\bar{H}}^a$  are small in the LEP 200 energy region. This allows us to include soft-photon exponentiation and  $\mathcal{O}(\alpha^2)$  leading-logarithmic corrections into the  $st$ - and  $t$ -channel universal terms, and to treat the nonuniversal rest to order  $\mathcal{O}(\alpha)$ .

At the beginning of this section we reproduced, in the context of off-shell  $W$ -pair production, a general result for  $s$ -channel ISR: the radiator functions  $\bar{S}$  and  $\bar{H}$ , which describe the creation of an intermediate vector boson  $V^*$  together with a photon,  $e^+e^- \rightarrow V^*(s')\gamma_{\text{ini}}$ . The corresponding  $t$ -channel contribution with two virtual vector bosons,

$$e^+e^- \rightarrow V_1^*(s_1)V_2^*(s_2)\gamma_{\text{ini}}, \quad (17)$$

and its interference with the  $s$  channel, is characterized mainly by the same, universal functions  $\bar{S}$  and  $\bar{H}$ , but also by some deviations  $\hat{S}$  and  $\hat{H}$ , due to the more involved kinematics. It was explicitly assumed that  $V_1^*$  and  $V_2^*$  have no common final-state interactions; such interactions would destroy the anticipated kinematical situation.

## 5 The Coulomb singularity

In the threshold region, there is another type of photonic corrections besides the ISR, which is potentially large: the Coulomb singularity [16]. For off-shell  $W$ -pair production, it originates in the  $s$  channel from the insertion of a virtual photon to the  $\gamma W^+ W^-$  and  $Z W^+ W^-$  vertices; in the  $t$  channel, it is due to the  $\nu W^+ W^- \gamma$  box diagram. It is not completely clear to us how to take the Coulomb singularity into account numerically, apart from the fact that it should appear as a universal, positive factor in the net cross section, which takes into account the off-shellness of the process and should approach the known on-shell correction,

$$\sigma_C = \sigma [1 + C(s'; s_1, s_2, M_W, \Gamma_W)], \quad (18)$$

$$C(s'; s_1, s_2, M_W, \Gamma_W \rightarrow 0) \xrightarrow{s_i \rightarrow M_W} \frac{\pi\alpha}{2\bar{\beta}(s')}, \quad \bar{\beta}(s') = \sqrt{1 - 4M_W^2/s'}. \quad (19)$$

With a Feynman-diagram calculation one may find the scalar one-loop function, in which the Coulomb singularity is located. Unfortunately, an evaluation of it without a knowledge of the kinematic behaviour of the imaginary part of the  $W$  propagator is impossible. A crude estimate, assuming for the  $W$ -propagators (4) under the loop integral that  $i\sqrt{s_i}\Gamma_W(s_i) \approx is_i\Gamma_W/M_W$ , yields for the leading term in the small-width approximation:

$$C(s'; s_1, s_2, M_W, \Gamma_W) = \left(1 - 3\frac{\Gamma_W^2}{M_W^2}\right) \frac{\pi\alpha}{2\bar{\beta}(s'; s_1, s_2)}, \quad \bar{\beta}(s'; s_1, s_2) = \frac{1}{s'} \sqrt{\lambda(s'; s_1, s_2)}. \quad (20)$$

Here,  $\lambda$  is the usual kinematic  $\lambda$ -function.

A different approach which is based on a non-relativistic treatment of the threshold region has been developed in [17, 18]. For details we refer to the original literature.

## 6 Numerical results

In the discussion of numerical results, we will concentrate on two observables, which may be used for a precise determination of the  $W$  mass at LEP 200 [4]. The calculations have been performed with the aid of the FORTRAN program **GENTLE** [19]. The corrected numerical values have been produced with version **CC11** of July 1995. We have used the following input parameter definitions, which slightly deviate from what was used in 1993:

$$\begin{aligned} G_\mu &= 1.16639 \times 10^{-5} \text{ GeV}^{-2}, \\ \alpha \equiv \alpha(2M_W) &= 1/128.07, \\ s_W^2 \equiv s_W^{2,eff} &= \frac{\pi\alpha}{\sqrt{2}G_\mu M_W^2}, \\ M_Z &= 91.1888 \text{ GeV}, \\ \Gamma_Z &= 2.49747, \end{aligned}$$

$$\begin{aligned}
M_W &= 80.230 \text{ GeV}, \\
\Gamma_W &= \frac{9G_\mu M_W^3}{6\pi\sqrt{2}}.
\end{aligned}
\tag{21}$$

We will discuss the radiative corrections both for the cases of on-shell and off-shell  $W$ -pair production. Our ‘minimal’ radiative corrections are the universal corrections introduced in (12), but neglecting the indicated terms of the order of  $\mathcal{O}(\alpha^2)$  [12]. Additionally, we may take into account:

- (i) the universal  $\mathcal{O}(\alpha^2)$  terms in (12) [ $U_2=0,1$ ];
- (ii) the nonuniversal cross sections  $\sigma_{\hat{S}}$  and  $\sigma_{\hat{H}}$  in (14) and (15), which are the main result of this study [ $\hat{S}=0,1$ ;  $\hat{H}=0,1$ ];
- (iii) the estimate of the Coulomb singularity (20) [ $C=0,1$ ].

## 6.1 The $W$ -pair excitation curve

We should like to start the discussion with a few comments on figure 4, where we show the cross sections  $\sigma_B^{\text{on}}$  and  $\sigma_B^{\text{off}}$  for Born on- and off-shell  $W$ -pair production, and also  $\sigma_T^{\text{off}}$  for the off-shell production with universal ISR ( $U_2=1$ ,  $\hat{S}=\hat{H}=C=0$ ). Compared to  $\sigma_B^{\text{on}}$ , the cross section  $\sigma_B^{\text{off}}$  develops a tail. Although this tail becomes heavily suppressed at high energies, it is not vanishing<sup>3</sup>. The other tail phenomenon is due to the universal ISR and is much more pronounced, but again weaker than e.g. is observed for the narrow  $Z$ -resonance shape. In the figure, the radiatively corrected on-shell cross section  $\sigma_T^{\text{on}}$  is not shown. As a matter of fact, we mention that the relative differences between  $\sigma_B^{\text{on}}$  and  $\sigma_B^{\text{off}}$ , and between  $\sigma_T^{\text{on}}$  and  $\sigma_T^{\text{off}}$  are quite similar.

Figure 5 and table 1 allow to estimate the differences between the simple universal ISR approximation and the exact treatment of ISR, which additionally includes the nonuniversal cross-section contributions connected with the **crab** diagram, and also the Coulomb singularity. The nonuniversal corrections  $\sigma_{\hat{S}}$  and  $\sigma_{\hat{H}}$  increase the total cross section by +0.4%; +0.8%; +1.5% at  $\sqrt{s} = 165 \div 190$ ; 500; 1000 GeV, respectively. We quote these values for the on-shell case; the off-shell corrections (in percent) are nearly the same.

On top of that, the Coulomb singularity yields a positive correction, which has its maximum value of about 6% at the threshold and asymptotically approaches the on-mass-shell value of  $\frac{1}{2}\pi\alpha = 1.15\%$ . At large  $\sqrt{s}$ , in contrast to the threshold region, it is only one of many  $\mathcal{O}(\alpha)$  corrections. We compared numerically our equation (20) with the predictions of equations (1) and (9)<sup>4</sup> of [18], and got very good agreement in the threshold region. The predictions of the non-relativistic calculation are slightly smaller, but the absolute differences of the two calculations do not exceed 0.5%.

## 6.2 The radiative energy loss

Two potential methods for a determination of  $M_W$  are the direct reconstruction of events and the measurement of the (upper and lower) energy end points in leptonic  $W$ -boson decays.

<sup>3</sup>In [9], with which we analytically agree, this is not seen from the figures.

<sup>4</sup>In equation (9) of [18], we treated the arctg as defined between 0 and  $\pi$ .



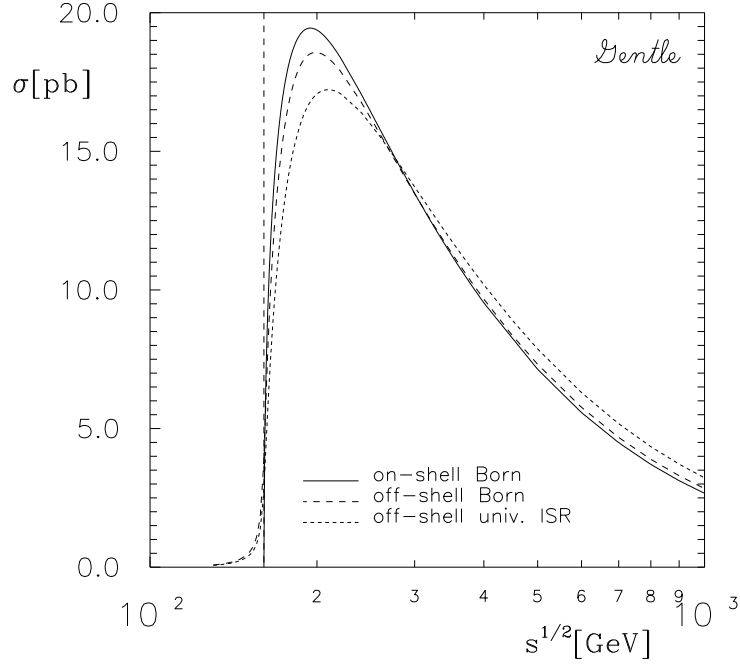


Figure 4: *Total cross section for  $W$ -pair production:  $\sigma_B$  and universal ISR corrections.*

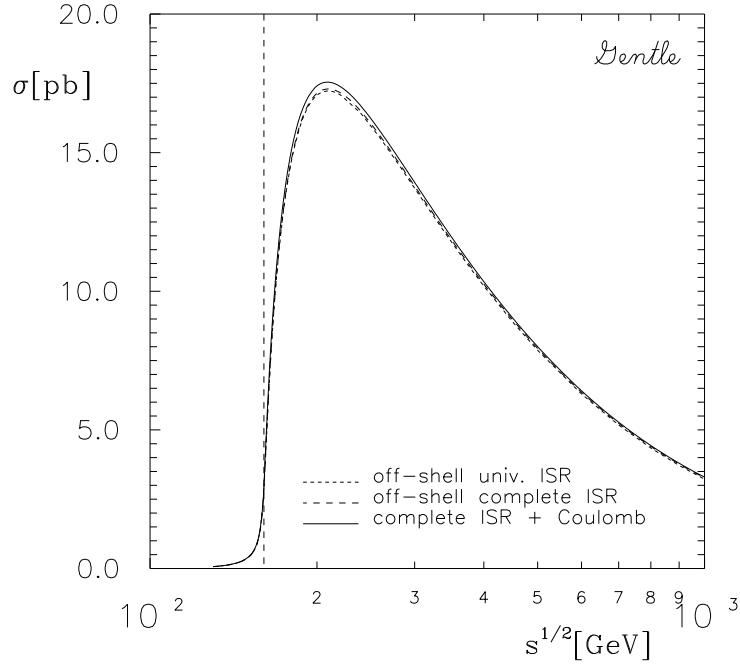


Figure 5: *Total cross section for  $W$ -pair production with ISR and Coulomb corrections.*

$\hat{S}$	$\hat{H}$	$U_2$	$C$	$\sigma$ , pb	$\langle E_{\text{rad}} \rangle$ , GeV
0	0	0	0	16.405	2.091
				13.634	1.158
0	0	1	0	16.401	2.153
				13.602	1.190
1	0	0	0	16.471	2.091
				13.686	1.159
0	1	0	0	16.405	2.090
				13.634	1.158
1	1	0	0	16.470	2.091
				13.686	1.159
0	0	0	1	16.783	2.107
				14.042	1.170
1	1	1	1	16.846	2.170
				14.063	1.201

Table 1: *The off-shell  $W$ -pair production cross section and the radiative energy loss at two energies:  $E_{\text{beam}}=95$  GeV (upper rows), 88 GeV (lower rows). The  $\hat{S}$  and  $\hat{H}$  switch on and off the soft and hard parts of the non-universal QED corrections, the  $U_2$  the second order corrections, and  $C$  the Coulomb correction.*

They both rely on the knowledge of the *effective* beam energy, which deviates from the beam energy itself by the radiative energy loss  $E_{\text{rad}}$ . Its average value is

$$\langle E_{\text{rad}} \rangle = \frac{1}{\sigma_T(s)} \int ds' k_0 \int ds_1 ds_2 \frac{d^3\sigma}{ds' ds_1 ds_2}, \quad (22)$$

$$k_0 = E_{n\gamma} = \frac{\sqrt{s}}{2} \left( 1 - \frac{s'}{s} \right). \quad (23)$$

Since the radiative energy loss is essentially due to ISR, with a possible smaller amount from initial-final interferences, one may assume that the formulae of the foregoing sections cover the bulk of effects.

Numerical estimates for the cross section and the radiative energy loss are collected in table 1 for two typical energies at LEP 200. The radiative energy loss amounts to about 2200 MeV at  $\sqrt{s}=190$  GeV (1200 MeV at  $\sqrt{s}=176$  GeV). These shifts are mainly due to the universal,  $\mathcal{O}(\alpha)$  ISR corrections with soft-photon exponentiation. Further, there are at 190 GeV shifts of +62;  $\pm 0$ ; +16 MeV due to: universal, non-exponentiated higher orders; nonuniversal corrections; the Coulomb singularity (at 176 GeV: +32;  $\pm 0$ ; +12 MeV, correspondingly). Apparently, these corrections have to be taken into account properly, if one aims at an accuracy of 50 to 100 MeV for the  $W$ -boson mass.

The numerical results of [20] were based on the corrected version of the Fortran program.

### 6.3 Conclusions

We have performed the first complete, gauge-invariant calculation of initial-state radiation corrections to off-shell  $W$ -pair production. In the threshold region, we also include the Coulomb singularity. The net improvements compared to the well-known universal ISR corrections are relatively small, but non-negligible, at LEP 200. They become more and more important at higher energies, and the final-state radiation seems to be much less pronounced after the inclusion of the auxiliary current into the ISR.

## Acknowledgements

We would like to thank W. Beenakker, A. Denner, F. Jegerlehner, W. Hollik, V. Khoze, R. Kleiss, G. van Oldenborgh, B. Pietrzyk for discussions. D.B. and T.R. gratefully acknowledge the hospitality at the MPI München, where part of the work has been performed.

We should like to thank D. Lehner who helped us finding a mistake in one of our SCHOONSCHIP codes for the calculation of the nonuniversal corrections.

## References

- [1] D. Bardin, S. Riemann and T. Riemann, *Z. Physik* **C32** (1986) 121;  
A. Denner and T. Sack, *Z. Physik* **C46** (1990) 653.
- [2] A. Sirlin, *Phys. Rev.* **D22** (1980) 213;  
D. Bardin et al., prepr. CERN-TH.6443/92, and references therein.

- [3] J. Ellis et al. (eds.), Physics at LEP, CERN 86-02 (1986);  
A. Böhm et al. (eds.), Proc. of the ECFA Workshop on LEP200, Aachen 1986, CERN 87-08 (1987).
- [4] L. Camilleri, presentation of the results of the working group on the  $W$  mass measurement at LEP 200, LEPC open session, CERN, 3 Nov. 1992, unpublished.
- [5] A. Aepli and D. Wyler, *Phys. Letters* **B262** (1991) 125;  
A. Aepli, preprint BNL-46819 (1991) and contribution to [8].
- [6] D. Bardin, M. Bilenky, A. Olchevski and T. Riemann, in preparation.
- [7] P. Zerwas (ed.), Proc. of the Workshop on  $e^+e^-$  Collisions at 500 GeV: The Physics Potential, Hamburg 1991, DESY 92-123B (1992).
- [8] P. Eerola et al. (eds.), Proc. of the Workshop on Physics and Experiments with Linear Colliders, Saariselkä, Finland, 1991 (World Scientific 1992).
- [9] T. Muta, R. Najima and S. Wakaizumi, *Mod. Phys. Letters* **A1** (1986) 203.
- [10] R. Kleiss, private communication;  
F. Berends and R. Kleiss, *Z. Physik* **C27** (1985) 365.
- [11] D. Bardin, C. Burdik, P. Christova and T. Riemann, *Z. Physik* **C44** (1989) 149.
- [12] F.A. Berends, G. Burgers and W.L. van Neerven, *Nucl. Phys.* **B297** (1988) 429;  
B. Kniehl, M. Krawczyk, J.H. Kühn and R. Stuart, *Phys. Letters* **B209** (1988) 337.
- [13] L.D. Landau and E.M. Lifschitz, Course of Theoretical Physics, Vol. IVb.
- [14] M. Veltman, program for algebraic manipulations **SCHOONSCHIP**;  
J. Vermaseren, program for algebraic manipulations **FORM**.
- [15] O. Sushkov, V. Flambaum and I. Khriplovich, *Sov. J. Nucl. Phys.* **20** (1975) 537;  
W. Alles, Ch. Boyer and A. Buras, *Nucl. Phys.* **B119** (1977) 125.
- [16] A. Sommerfeld, "Atombau und Spektrallinien", Band 2 (Vieweg, Braunschweig, 1959);  
A.D. Sakharov, *JETP* **18** (1948) 631.
- [17] V. Fadin and V. Khoze, *JETP Letters* **46** (1987) 417; *Yad. Phys.* **48** (1988) 487.
- [18] V. Fadin, V. Khoze and A. Martin, Durham preprint DTP/93/06 (1993).
- [19] D. Bardin, M. Bilenky, A. Olchevski and T. Riemann, FORTRAN program **GENTLE**:  
A semi-Monte Carlo **GEN**erator of the radiative Tail for LEP 200.
- [20] D. Bardin, M. Bilenky, A. Olchevski and T. Riemann, contrib. to: P. Zerwas (ed.), Proceedings of the Workshop on  $e^+e^-$  Collisions at 500 GeV: the Physics Potential, Munich, Annecy, Hamburg, 20 Nov 1992 - 3 Apr 1993, DESY 93-123C (Dec. 1993) 159-164.